


**Boosting the performance of quantum Otto heat engines**Jin-Fu Chen,<sup>1,2</sup> Chang-Pu Sun,<sup>1,2</sup> and Hui Dong<sup>2,\*</sup><sup>1</sup>*Beijing Computational Science Research Center, Beijing 100193, China*<sup>2</sup>*Graduate School of China Academy of Engineering Physics, No. 10 Xibeiwang East Road, Haidian District, Beijing, 100193, China* (Received 5 August 2019; revised manuscript received 12 September 2019; published 30 September 2019)

To optimize the performance of a heat engine in a finite-time cycle, it is important to understand the finite-time effect of thermodynamic processes. Previously, we have shown that extra work is needed to complete a quantum adiabatic process in finite time, and proved that the extra work follows a  $C/\tau^2$  scaling for long control time  $\tau$ . There the oscillating part of the extra work is neglected due to the complex energy-level structure of the particular quantum system. However, such oscillation of the extra work cannot be neglected in some quantum systems with simple energy-level structure, e.g., the two-level system or the quantum harmonic oscillator. In this paper, we build the finite-time quantum Otto engine on these simple systems, and find that the oscillating extra work leads to a jagged edge in the constraint relation between the output power and the efficiency. By optimizing the control time of the adiabatic processes, the oscillation in the extra work is utilized to enhance the maximum power and the efficiency. We further design special control schemes with the zero extra work at the specific control time. Compared to the linear control scheme, these special control schemes of the finite-time adiabatic process improve the maximum power and the efficiency of the finite-time Otto engine.

DOI: [10.1103/PhysRevE.100.032144](https://doi.org/10.1103/PhysRevE.100.032144)**I. INTRODUCTION**

Quantum thermodynamics [1–5] studies the effect of quantum characteristics, e.g., coherence [6–9], entanglement [10–13], and quantum many-body effects [14–17], on the thermodynamic property of the system. One important topic is to find quantum heat engines as counterparts of the classical ones. To design a practical heat engine with nonzero output power, the finite-time quantum thermodynamics [18–23] needs to be studied instead of quasistatic thermodynamics [15–17,24]. Therefore understanding the finite-time effect of thermodynamic processes is crucial to the optimization of the finite-time heat engine [22,25–29]. Based on the universal  $C/\tau$  scaling of the entropy production in finite-time isothermal processes [19], the efficiency at maximum power is obtained analytically for the finite-time Carnot-like engine [18,20,30,31]. The tradeoff relation between efficiency and power was further established recently [28,32–36] for the finite-time Carnot cycle. The finite-time heat engine of other types, e.g., the finite-time Otto engine, has been studied [27,29,37–45] and is shown with better performance by the technique of the shortcut to adiabatic [46–53]. Yet, the optimization of the finite-time Otto engine lacks a general principle compared to the universal  $C/\tau$  scaling of the entropy production in the finite-time Carnot-like engine.

Evaluating the finite-time effect of adiabatic processes is the key to the optimization of the finite-time Otto engine, which consists of two finite-time adiabatic processes and two finite-time isochoric processes. We consider the situation where the time consumption of the finite-time isochoric processes can be neglected compared to that of the finite-time

adiabatic processes [50,54]. During the finite-time adiabatic process, the system is isolated from the environment and evolves under the time-dependent Hamiltonian [55]. When energy levels of different states do not cross, the quantum adiabatic approximation is valid for long control time [24]. In this situation, the theorem of high-order adiabatic approximation provides a perturbative technique to derive the finite-time correction to higher orders of the inverse control time [56–59]. It requires positive extra work to complete the quantum adiabatic process in finite time.

In our previous paper [60], we found that the extra work in the finite-time adiabatic process can be naturally divided into the mean extra work and the oscillating extra work. With the increasing control time  $\tau$ , the mean extra work decreases monotonously, obeying a general  $C/\tau^2$  scaling behavior. The oscillating extra work oscillates around zero for larger  $\tau$ , and is neglected due to the incommensurable energy of different states in large systems. Yet, this oscillating extra work cannot be neglected for the system with a simple energy-level structure. In this paper, we continue the study of the oscillating extra work, and show its effects on some simple systems, such as the two-level system and the quantum harmonic oscillator. We find that the oscillation of the extra work can be utilized to enhance the output power of the heat engine. Besides, we obtain special control schemes of the finite-time adiabatic processes with zero extra work at the specific control time. The special control scheme further improves the maximum power of the Otto engine.

This paper is organized as follows. In Sec. II, we review the generic finite-time quantum Otto engine, and list the dependence of the power and the efficiency on the extra work in the finite-time adiabatic processes for later discussion. In Secs. III and IV, the finite-time quantum Otto cycles on

\*hdong@gascaep.ac.cn

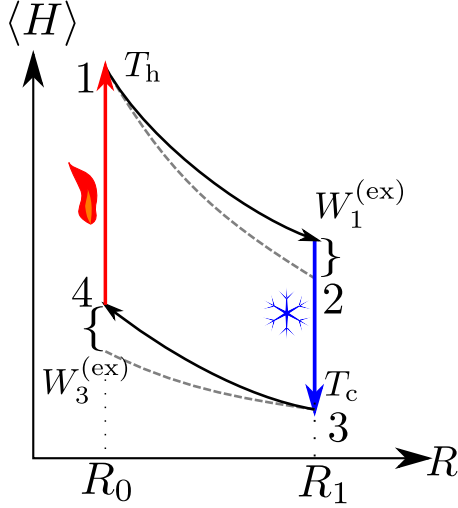


FIG. 1. Energy-parameter ( $\langle H \rangle - R$ ) diagram of the finite-time Otto cycle. The solid line with arrows presents the finite-time cycle, where two vertical colored lines present the isochoric processes (red for heating and blue for cooling), and two black lines present the finite-time adiabatic processes. The dashed lines present the quantum adiabatic processes. The extra work in the two finite-time adiabatic processes is marked as  $W_1^{(ex)}(\tau_1)$  and  $W_3^{(ex)}(\tau_3)$ .

two-level systems and quantum harmonic oscillators are studied, respectively. The conclusion is given in Sec. V.

## II. FINITE-TIME QUANTUM OTTO ENGINE

In this section, we briefly review the finite-time Otto cycle. A generic finite-time Otto cycle consists of four strokes, two finite-time adiabatic processes and two finite-time isochoric processes, illustrated by the  $\langle H \rangle - R$  diagram in Fig. 1. We consider the relaxation time in the isochoric process as much shorter than the time consumption of the finite-time adiabatic process. The time consumed by the isochoric process can be neglected, and the initial state of the finite-time adiabatic process can be regarded as a thermal state.

In the finite-time adiabatic processes ( $1 \rightarrow 2$  and  $3 \rightarrow 4$ ) with the control time  $\tau_1$  and  $\tau_3$ , the system is isolated from any baths so that the thermodynamic adiabaticity is satisfied. The work is performed by tuning the parameter  $R(t)$  in the Hamiltonian  $H(t) \equiv H[R(t)]$ , from  $R_0$  to  $R_1$  in the process  $1 \rightarrow 2$  and inversely in  $3 \rightarrow 4$ . The system evolves under the time-dependent Hamiltonian as  $\dot{\rho} = -i[H(t), \rho]$ . The work done for the finite-time adiabatic process equals the change of the internal energy

$$W(\tau) = \text{Tr}[\rho(\tau)H(\tau)] - \text{Tr}[\rho(0)H(0)], \quad (1)$$

where  $\tau$  is the control time of the adiabatic process. The initial state  $\rho(0)$  is a thermal state, while the final state  $\rho(\tau)$  is not necessarily a thermal state. The finite-time adiabatic process requires more work than the quantum adiabatic one. In Ref. [60], we rewrite the work as

$$W(\tau) = W^{\text{adi}} + W^{(\text{ex})}(\tau), \quad (2)$$

where  $W^{\text{adi}}$  is the work done in the quantum adiabatic process with infinite control time, and  $W^{(\text{ex})}(\tau)$  is the extra work for the finite-time adiabatic process.

We have shown that the extra work can be naturally divided into the mean extra work and the oscillating extra work

$$W^{(\text{ex})}(\tau) = W^{(\text{mean})}(\tau) + W^{(\text{osc})}(\tau). \quad (3)$$

The mean extra work decreases monotonously for longer control time  $\tau$ , satisfying the  $\mathcal{C}/\tau^2$  scaling behavior. The oscillating extra work oscillates around zero with the increasing control time. For a large and complicated physical system, the oscillating extra work is usually neglected due to the incommensurable energy levels of different states [60]. However, in quantum systems with simple energy-level structures, the contribution of the oscillating extra work should be taken into account.

To evaluate the efficiency, one needs to obtain the heat transfer in the isochoric process  $4 \rightarrow 1$  ( $2 \rightarrow 3$ ). Since no work is performed in this process, the heat is determined by the change of the internal energy. In the process  $4 \rightarrow 1$ , the system absorbs the heat from the hot source  $Q_h = \langle H \rangle_1 - \langle H \rangle_4 > 0$ , while the system releases the heat to the cold sink  $Q_c = \langle H \rangle_3 - \langle H \rangle_2 < 0$  in the process  $2 \rightarrow 3$ . The time consumption of the isochoric process can be neglected compared to that of the adiabatic process [50,54]. For a whole cycle, the net work is  $W_T = Q_h - |Q_c|$  with the efficiency  $\eta = W_T/Q_h$ .

In Ref. [60], we have obtained the power

$$P = \frac{W_T^{\text{adi}} - W_1^{(\text{ex})}(\tau_1) - W_3^{(\text{ex})}(\tau_3)}{\tau_1 + \tau_3} \quad (4)$$

and the efficiency

$$\eta = \frac{W_T^{\text{adi}} - W_1^{(\text{ex})}(\tau_1) - W_3^{(\text{ex})}(\tau_3)}{Q_h^{\text{adi}} - W_3^{(\text{ex})}(\tau_3)} \quad (5)$$

for the finite-time Otto cycle. Here,  $W_T^{\text{adi}}$  and  $Q_h^{\text{adi}}$  denote the net work and the heat absorbed from the hot source in the quasistatic Otto cycle.  $W_1^{(\text{ex})}(\tau_1)$  and  $W_3^{(\text{ex})}(\tau_3)$  denote the extra work for the finite-time adiabatic processes  $1 \rightarrow 2$  and  $3 \rightarrow 4$  respectively. For given control times  $\tau_1$  and  $\tau_3$ , higher power and efficiency can be achieved by optimizing the protocol to reduce the extra work  $W_1^{(\text{ex})}(\tau_1)$  and  $W_3^{(\text{ex})}(\tau_3)$ .

In the previous paper, the constraint relation between the efficiency and the output power is obtained by neglecting the oscillating extra work for the system with complex energy-level structure. We only consider the mean part in the extra work  $W_1^{(\text{ex})}(\tau_1) \approx \Sigma_1/\tau_1^2$  and  $W_3^{(\text{ex})}(\tau_3) \approx \Sigma_3/\tau_3^2$ , where  $\Sigma_1$  ( $\Sigma_3$ ) is the coefficient determined by the control scheme of the finite-time adiabatic process  $1 \rightarrow 2$  ( $3 \rightarrow 4$ ) [60]. The efficiency at the maximum power follows as

$$\eta_{\text{EMP}} = \frac{2\eta^{\text{adi}}}{3 - \eta^{\text{adi}}/[1 + (\Sigma_1/\Sigma_3)^{1/3}]}, \quad (6)$$

where  $\eta^{\text{adi}}$  is the efficiency of the quasistatic Otto cycle. Yet such simplification fails for a quantum system with a simple energy-level structure. We will explore the effect of the oscillating extra work for the simple quantum system in the following section.

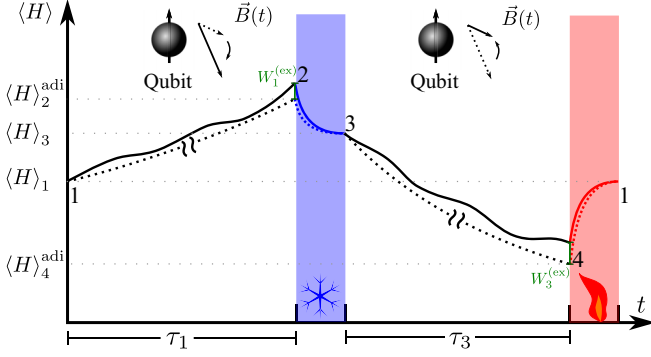


FIG. 2. Finite-time Otto cycle of the two-level system. The magnetic field  $\vec{B}(t)$  is modulated in the finite-time adiabatic process. Similar to Fig. 1, the solid line presents the finite-time cycle, with the dashed line for the quasistatic one plotting for comparison. The time consumed by the two adiabatic processes is  $\tau_1$  and  $\tau_3$ , while the time consumed by the isochoric processes is neglected.

### III. TWO-LEVEL OTTO ENGINE

To show the effect of the oscillating extra work, we start with the simplest model of a two-level system, a spin in a controllable magnetic field  $\vec{B}(t)$ . The Hamiltonian of the system reads

$$H = \mu \vec{B}(t) \cdot \vec{\sigma}, \quad (7)$$

with the magnetic moment  $\mu$  and the Pauli matrix  $\vec{\sigma}$ . We consider the magnetic field is modulated as  $\vec{B}(t) = [B_z(t) + B_\theta \cos \theta] \vec{e}_z + B_\theta \sin \theta \vec{e}_x$  in the finite-time adiabatic process, where  $\theta$  is the angle of the static magnetic field  $B_\theta$ . With the ratio of the magnetic field  $\lambda = B_z(t)/B_\theta$ , the Hamiltonian of the two-level system [27] is rewritten as

$$H = \epsilon [(\lambda - \cos \theta) \sigma_z + \sin \theta \sigma_x], \quad (8)$$

by setting  $\epsilon = \mu B_\theta$  as the unit of the energy. Here,  $\lambda = \lambda(t)$  serves as the tuning parameter  $R(t)$  in the finite-time adiabatic process. Figure 2 shows the finite-time Otto cycle realized on the two-level system. We present the finite-time cycle with the solid curve, and the quasistatic cycle with the dashed curve. In the two isochoric processes, the magnetic field is fixed and the system contacts with the hot source or the cold sink and reaches equilibrium (the red and blue curves).

To apply the high-order adiabatic approximation, we rewrite the Hamiltonian under the basis of instantaneous eigenstates [56] as

$$H = \epsilon \Lambda(t) [|e(t)\rangle \langle e(t)| - |g(t)\rangle \langle g(t)|], \quad (9)$$

where the instantaneous eigenenergy  $\epsilon \Lambda(t)$  is determined by  $\lambda(t)$  as

$$\Lambda(t) = \sqrt{\lambda^2 - 2\lambda \cos \theta + 1}. \quad (10)$$

The instantaneous ground state is

$$|g(t)\rangle = 1/N_1 \begin{pmatrix} \lambda - \cos \theta - \Lambda \\ \sin \theta \end{pmatrix}, \quad (11)$$

and the instantaneous excited state is

$$|e(t)\rangle = 1/N_2 \begin{pmatrix} \lambda - \cos \theta + \Lambda \\ \sin \theta \end{pmatrix}, \quad (12)$$

where  $N_1 = [2\Lambda(\Lambda - \lambda + \cos \theta)]^{1/2}$  and  $N_2 = [2\Lambda(\Lambda + \lambda - \cos \theta)]^{1/2}$  are the normalized factors.

The initial state is a thermal state  $\rho(0) = p_g |g(0)\rangle \langle g(0)| + p_e |e(0)\rangle \langle e(0)|$ , where the distribution is  $p_g = 1 - p_e = 1/[1 + \exp(-2\beta\epsilon\Lambda(0))]$  with the inverse temperature  $\beta$ . The density matrix at any time  $t \in [0, \tau]$  is  $\rho(t) = p_g |\psi_g(t)\rangle \langle \psi_g(t)| + p_e |\psi_e(t)\rangle \langle \psi_e(t)|$ , where the state  $|\psi_n(t)\rangle$ ,  $n = e, g$  obeys the Schrödinger equation

$$i\partial_t |\psi_n(t)\rangle = H(t) |\psi_n(t)\rangle, \quad (13)$$

with the initial condition  $|\psi_n(0)\rangle = |n(0)\rangle$ . We express the state under the basis of the instantaneous eigenstates

$$|\psi_n(t)\rangle = c_{ng}(t) e^{i\phi(t)} |g(t)\rangle + c_{ne}(t) e^{-i\phi(t)} |e(t)\rangle \quad (14)$$

with the dynamical phase  $\phi(t) = \epsilon \int_0^t \Lambda(t') dt'$ . The Schrödinger equation by Eq. (13) gives the differential equations

$$\dot{c}_{ng} = e^{-2i\phi} \frac{\sin |\theta| \dot{\lambda}}{2\Lambda^2} c_{ne}, \quad (15)$$

and

$$\dot{c}_{ne} = -e^{2i\phi} \frac{\sin |\theta| \dot{\lambda}}{2\Lambda^2} c_{ng}. \quad (16)$$

We consider a given protocol  $\tilde{\lambda}(s) = \lambda(s\tau)$  with adjustable control time  $\tau$ , where  $s = t/\tau \in [0, 1]$  denotes the rescaled time parameter. The internal energy at the end of the finite-time adiabatic process is  $\langle H(\tau) \rangle = (p_e - p_g)[1 - 2|c_{eg}(\tau)|^2] \epsilon \tilde{\Lambda}(1)$  with the notation  $\tilde{\Lambda}(s) = \Lambda(s\tau)$ . Together with Eqs. (1) and (2), we obtain the quasistatic work

$$W^{\text{adi}} = -\epsilon \tanh[\beta\epsilon \tilde{\Lambda}(0)] [\tilde{\Lambda}(1) - \tilde{\Lambda}(0)], \quad (17)$$

and the extra work for the finite-time adiabatic process

$$W^{(\text{ex})}(\tau) = 2\epsilon \tilde{\Lambda}(1) \tanh[\beta\epsilon \tilde{\Lambda}(0)] |c_{ge}(\tau)|^2. \quad (18)$$

At long control time limit, the first-order adiabatic approximation gives the asymptotic amplitude for Eq. (16)

$$c_{ge}^{[1]}(\tau) = \frac{i \sin |\theta|}{4\epsilon\tau} \left( \frac{\tilde{\lambda}'(1)}{\tilde{\Lambda}(1)^3} e^{2i\tau\tilde{\phi}(1)} - \frac{\tilde{\lambda}'(0)}{\tilde{\Lambda}(0)^3} \right), \quad (19)$$

where the dynamical phase is rewritten as  $\tilde{\phi}(s) = \epsilon \int_0^s \tilde{\Lambda}(s') ds'$ , and  $\tilde{\lambda}'(s) = d\tilde{\lambda}(s)/ds$  denotes the derivative of  $\tilde{\lambda}(s)$ . The derivation of Eq. (19) is given in Appendix A. Substituting Eq. (19) into the extra work by Eq. (18), the asymptotic extra work is naturally divided into two parts according to Eq. (3): the mean extra work

$$W^{\text{(mean)}} = \frac{\sin^2 \theta \tilde{\Lambda}(1)}{8\epsilon\tau^2} \left( \frac{\tilde{\lambda}'(1)^2}{\tilde{\Lambda}(1)^6} + \frac{\tilde{\lambda}'(0)^2}{\tilde{\Lambda}(0)^6} \right) \tanh[\beta\epsilon \tilde{\Lambda}(0)], \quad (20)$$

and the oscillating extra work

$$W^{\text{(osc)}} = -\frac{\sin^2 \theta \tilde{\lambda}'(1) \tilde{\lambda}'(0) \cos[2\tau\tilde{\phi}(1)]}{4\epsilon\tau^2 \tilde{\Lambda}(1)^2 \tilde{\Lambda}(0)^3} \tanh[\beta\epsilon \tilde{\Lambda}(0)]. \quad (21)$$

To obtain the efficiency and the power for the finite-time Otto cycle, we need the net work  $W_T^{\text{adi}}$  and the heat absorbed  $Q_h^{\text{adi}}$  in the quasistatic Otto cycle with the

infinite control time  $\tau \rightarrow \infty$ . The magnetic field  $B_z(t)$  is modulated from  $B_0$  to  $B_1$  in the finite-time adiabatic process  $1 \rightarrow 2$ , with the corresponding parameter  $\lambda_0$  and  $\lambda_1$  at the initial and final time. Since the population on the excited state remains unchanged during the quantum adiabatic processes [24], the internal energy of the four states follows immediately as  $\langle H \rangle_1 = -E_0 \tanh(\beta_h E_0)$ ,  $\langle H \rangle_2^{\text{adi}} = -E_1 \tanh(\beta_h E_0)$ ,  $\langle H \rangle_3 = -E_1 \tanh(\beta_c E_1)$ , and  $\langle H \rangle_4^{\text{adi}} = -E_0 \tanh(\beta_c E_1)$ . Here,  $\beta_l = 1/k_B T_l$  is the inverse temperature for the hot source ( $l = h$ ) and the cold sink ( $l = c$ ), and  $E_j = \epsilon \sqrt{\lambda_j^2 - 2\lambda_j \cos \theta + 1}$ ,  $j = 0, 1$  gives the abbreviation of the eigenenergy. The net work of the quasistatic Otto cycle is

$$W_T^{\text{adi}} = (E_0 - E_1)[\tanh(\beta_c E_1) - \tanh(\beta_h E_0)]. \quad (22)$$

The heat absorbed from the hot source is

$$Q_h^{\text{adi}} = E_0[\tanh(\beta_c E_1) - \tanh(\beta_h E_0)]. \quad (23)$$

The efficiency of the quasistatic Otto cycle is  $\eta^{\text{adi}} = 1 - E_1/E_0$  [24]. For the finite-time Otto cycle, the power and the efficiency are obtained by substituting the extra work by Eq. (18) and the quasistatic net work and heat by Eqs. (22) and (23) into Eqs. (4) and (5), respectively.

We compare the asymptotic extra work by Eqs. (20) and (21) with the exact numerical result in Fig. 3(a). The exact numerical result is obtained by numerically solving Eqs. (15) and (16). We choose the parameters  $\theta = 0.4$ ,  $\epsilon = 1$ ,  $\lambda_0 = 0.1$ ,  $\lambda_1 = 0.8$ , and set temperatures for the hot source and cold sink as  $k_B T_h = 5$  and  $k_B T_c = 2$ . We first adopt the linear protocol  $\tilde{\lambda}_l(t/\tau_1) = \tilde{\lambda}(0) + [\tilde{\lambda}(1) - \tilde{\lambda}(0)]t/\tau_1$ . Figure 3(a) shows the extra work for the finite-time adiabatic process  $1 \rightarrow 2$  with different control time  $\tau_1$ , where the initial and the final tuning parameters are  $\tilde{\lambda}(0) = \lambda_0$  and  $\tilde{\lambda}(1) = \lambda_1$ . The extra work (the blue curve) decreases with oscillation with the increasing control time, satisfying the  $C/\tau^2$  scaling (the red dashed line). The asymptotic extra work from the first-order adiabatic approximation (the green dotted curve) matches with the exact numerical result (the blue curve) at long control time.

We evaluate the performance of the finite-time Otto engine by modulating the control time  $\tau_1$  and  $\tau_3$  for the finite-time adiabatic processes. Figure 3(b) illustrates the constraint relation between efficiency and power. The red area presents the result with the mean extra work  $W^{(\text{mean})}(\tau)$ , where the oscillating extra work is neglected. The blue dots present the exact numerical result of the efficiency and power with the given pair of the control time  $(\tau_1, \tau_3)$  for two adiabatic processes. To obtain a clear boundary on the efficiency and power diagram, we sample the control time exponentially as  $(\tau_1, \tau_3) = a(r^{j_1}, r^{j_2})$  with the shortest control time  $a$ . The ratio  $r$  is set as 1.03 for all the efficiency and power diagrams in this paper. In Fig. 3(b), the shortest control time is  $a = 0.125$ .  $j_1$  and  $j_2$  are the integers ranging from 0 to 300, which leads to a distribution of the control time ranging from 0.125 to 887. Fig. 3(b) shows that the oscillation of the extra work leads to a jagged edge in the constraint relation, and can be utilized to achieve larger maximum power.

To attain high power, we should reduce the extra work in the finite-time adiabatic processes at the given control time

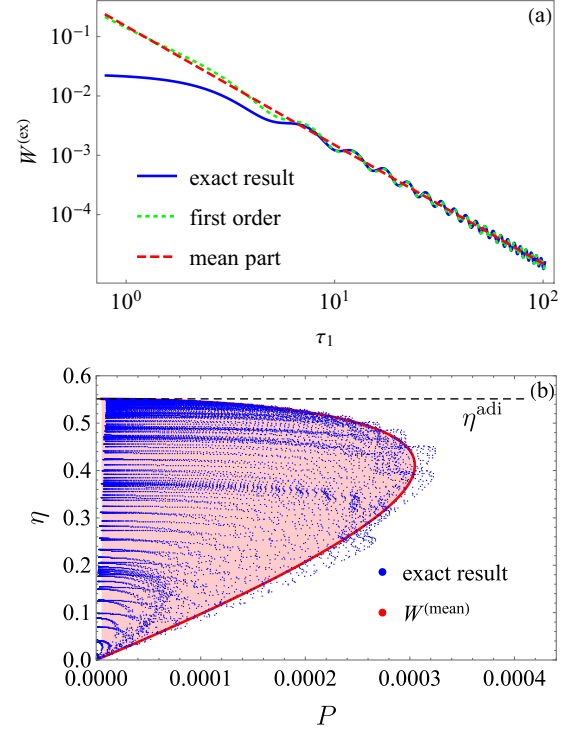


FIG. 3. (a) Extra work for the finite-time adiabatic process  $1 \rightarrow 2$  with the linear protocol  $\tilde{\lambda}_l$ . The blue solid curve, green dotted curve, and red dashed line present the exact numerical result, the first-order adiabatic result, and the mean extra work, respectively, while the horizontal black dashed line presents the quasistatic efficiency. The parameters are chosen as  $\lambda_0 = 0.1$  and  $\lambda_1 = 0.8$  with  $\theta = 0.4$  and  $\epsilon = 1$ , with the temperatures  $T_h = 5$  and  $T_c = 2$ . (b) Reachable power and efficiency for the finite-time two-level Otto engine. Each blue dot corresponds to a pair of control times  $(\tau_1, \tau_3)$  of two adiabatic processes. The red area only accounts for the mean extra work, while the blue dots present the exact numerical result.

$\tau_1$  or  $\tau_3$ . The extra work by Eqs. (20) and (21) approaches zero at the specific control time  $\tau = n\pi/\tilde{\phi}(1)$ ,  $n = 1, 2, \dots$  with the condition  $\tilde{\lambda}'(1)/[\tilde{\Lambda}(1)]^3 = \tilde{\lambda}'(0)/[\tilde{\Lambda}(0)]^3$ . We design a special protocol  $\tilde{\lambda}_s(s)$  to satisfy this condition, determined by the implicit equation

$$s = \frac{\frac{\tilde{\lambda}(s) - \cos \theta}{\tilde{\Lambda}(s)} - \frac{\tilde{\lambda}(0) - \cos \theta}{\tilde{\Lambda}(0)}}{\frac{\tilde{\lambda}(1) - \cos \theta}{\tilde{\Lambda}(1)} - \frac{\tilde{\lambda}(0) - \cos \theta}{\tilde{\Lambda}(0)}}. \quad (24)$$

By adopting this special protocol for the finite-time adiabatic processes, the efficiency of the Otto cycle approaches the quasistatic one  $\eta^{\text{adi}} = W_T^{\text{adi}}/Q_h^{\text{adi}}$  with finite output power.

Figure 4(a) presents the first-order adiabatic extra work (the green dotted curve), the mean extra work (the red dashed line) and the exact one (the blue solid curve) for the designed protocol by Eq. (24). The extra work for the linear protocol (the black dash-dotted curve) is plotted for comparison. The dynamical phase of the special protocol is  $\tilde{\phi}(1) = 0.531$ , obtained by Eq. (A5) in Appendix A. Hence, the extra work approaches zero at the specific control time  $\tau = n\pi/\tilde{\phi}(1) = n \times 5.92$ ,  $n = 1, 2, \dots$ , shown as the vertical gray line.

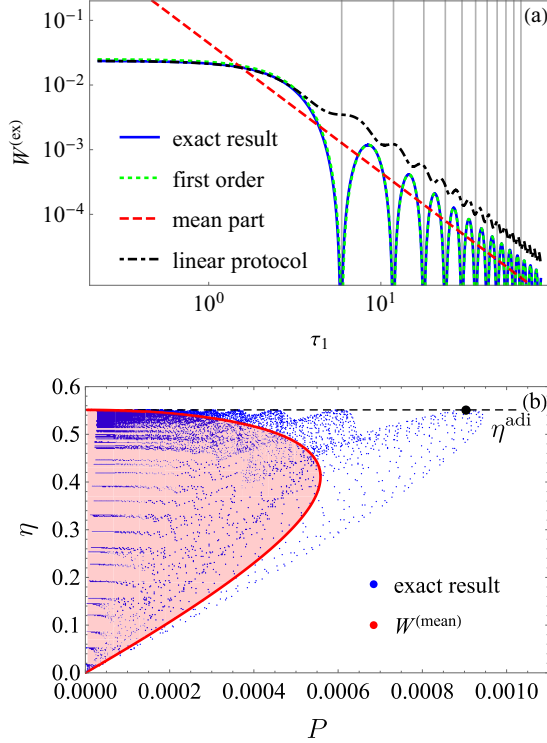


FIG. 4. (a) Extra work for the finite-time adiabatic process  $1 \rightarrow 2$  with the special protocol  $\tilde{\lambda}_s$  by Eq. (24). The black dash-dotted curve presents the exact extra work in the previous linear protocol for comparing. The vertical gray line shows that the extra work approaches zero at the specific control time. (b) Reachable power and efficiency with the special protocol. The horizontal dashed line presents the quasistatic  $\eta^{adi} = 0.551$ . The same parameters are chosen as in Fig. 3.

Figure 4(b) presents the constraint relation between the efficiency and the power for the special protocol. We use the same sampling of the control times  $\tau_1$  and  $\tau_3$  as that in Fig. 3(b). When the control time of the two adiabatic processes is chosen as the specific control time  $\tau = n\pi/\tilde{\phi}(1)$ , the efficiency approaches the quasistatic efficiency  $\eta^{adi} = 0.551$  (the horizontal black dashed line). For the specific control time  $\tau_1 = \tau_3 = 5.92$ , the heat engine gains large power with the quasistatic efficiency, marked with the black point. Compared to the linear protocol, the quantum Otto engine with the special protocol attains larger maximum power and the higher efficiency.

By optimizing the control time of the adiabatic processes, the oscillating extra work can be utilized to improve the maximum power and the efficiency for the finite-time Otto engine. In the next section, we continue to study the effect of similar oscillation of the extra work on the Otto cycle with a quantum harmonic oscillator.

#### IV. QUANTUM HARMONIC OTTO ENGINE

Another system with a simple energy level structure is the quantum harmonic oscillator, which has been widely studied as a prototype of the quantum Otto engine [29,40,42]. The technique of a shortcut to adiabaticity has been applied to ameliorate the quantum harmonic Otto engine [46,47,50,53].

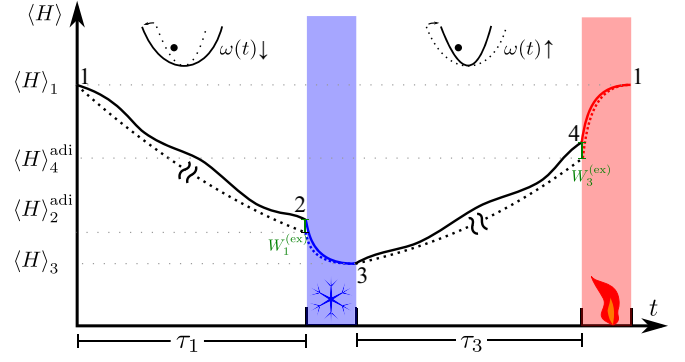


FIG. 5. Finite-time Otto cycle of the quantum harmonic oscillator. The frequency  $\omega(t)$  of the oscillator is modulated in the finite-time adiabatic process.

Here, we consider a generic finite-time adiabatic process described by the time-dependent Hamiltonian

$$H = -\frac{1}{2M} \frac{\partial^2}{\partial x^2} + \frac{1}{2} M \omega^2 x^2. \quad (25)$$

The frequency  $\omega = \omega(t)$ ,  $t \in [0, \tau]$  serves as the tuning parameter in the finite-time adiabatic process. The wave function of the instantaneous eigenstate is

$$\langle x|n(t)\rangle = N_n \exp\left(-\frac{1}{2} M \omega x^2\right) H_n(\sqrt{M\omega}x), \quad (26)$$

with the corresponding instantaneous eigenenergy  $E_n(t) = (n + 1/2)\omega(t)$ .  $H_n(\xi) = (-1)^n \exp(\xi^2) \partial^n / \partial \xi^n [\exp(-\xi^2)]$  denotes the Hermite polynomial with the order  $n$ , and  $N_n = (\sqrt{M\omega}/\sqrt{\pi}2^n n!)^{1/2}$  is the normalized factor.

Figure 5 illustrates the finite-time quantum harmonic Otto cycle. Similar to the Otto cycle of the two-level system, the work is performed in two adiabatic processes  $1 \rightarrow 2$  and  $3 \rightarrow 4$ , while the system exchanges the heat with the hot source (cold sink) and reaches equilibrium in the isochoric process  $4 \rightarrow 1$  ( $2 \rightarrow 3$ ).

In the two adiabatic processes  $1 \rightarrow 2$  and  $3 \rightarrow 4$ , the initial state is the thermal state  $\rho(0) = \sum_{n=0}^{\infty} p_n |n(0)\rangle \langle n(0)|$  with the distribution  $p_n = 2 \sinh[\beta\omega(0)/2] \exp[-\beta(n + 1/2)\omega(0)]$ . The density matrix at any time  $t$  during the evolution is  $\rho(t) = \sum_{n=0}^{\infty} p_n |\psi_n(t)\rangle \langle \psi_n(t)|$ . Here, the state  $|\psi_n(t)\rangle$ ,  $n = 0, 1, 2, \dots$  obeys the Schrödinger equation  $i\partial_t |\psi_n(t)\rangle = H(t) |\psi_n(t)\rangle$ , with the initial condition  $|\psi_n(0)\rangle = |n(0)\rangle$ . Similar to Eq. (9), we rewrite the state under the instantaneous diagonal basis

$$|\psi_n(t)\rangle = \sum_m c_{nm}(t) e^{-i(m+\frac{1}{2})\varphi(t)} |n(t)\rangle, \quad (27)$$

with the dynamical phase  $\varphi(t) = \int_0^t \omega(t') dt'$ . The differential equation of  $c_{nm}(t)$  is obtained in Appendix B.

To evaluate the finite-time effect of the adiabatic process, we consider a protocol  $\tilde{\omega}(s) = \omega(s\tau)$  with adjustable control time  $\tau$ , with the instantaneous energy as  $\tilde{E}_n(s) = E_n(s\tau)$ . We rewrite the work into the quasistatic work and the extra work as Eq. (2). The quasistatic work with infinite control time

$\tau \rightarrow \infty$  is

$$W^{\text{adi}} = \sum_{n=0}^{\infty} p_n [\tilde{E}_n(1) - \tilde{E}_n(0)], \quad (28)$$

while extra work in the finite-time adiabatic process is

$$W^{(\text{ex})}(\tau) = \sum_{n,m=0}^{\infty} p_n |c_{nm}(\tau)|^2 [\tilde{E}_m(1) - \tilde{E}_n(1)]. \quad (29)$$

Similar to Eq. (19), the asymptotic amplitude at long control time is given by the first-order adiabatic approximation

$$c_{n,n+2}^{[1]}(\tau) = -i \frac{\sqrt{(n+1)(n+2)}}{8\tau} \left[ \frac{\tilde{\omega}'(1)}{\tilde{\omega}(1)^2} e^{2i\tau\tilde{\varphi}(1)} - \frac{\tilde{\omega}'(0)}{\tilde{\omega}(0)^2} \right], \quad (30)$$

and

$$c_{n,n-2}^{[1]}(\tau) = -i \frac{\sqrt{n(n-1)}}{8\tau} \left[ \frac{\tilde{\omega}'(1)}{\tilde{\omega}(1)^2} e^{-2i\tau\tilde{\varphi}(1)} - \frac{\tilde{\omega}'(0)}{\tilde{\omega}(0)^2} \right], \quad (31)$$

where the dynamical phase factor is  $\tilde{\varphi}(1) = \int_0^1 \tilde{\omega}(s) ds$ . The derivation of Eqs. (30) and (31) is given in Appendix B. The terms  $c_{nm}^{[1]}(\tau)$ ,  $m \neq n$ ,  $n \pm 2$  are all zero in the first-order adiabatic approximation. According to Eq. (3), the asymptotic extra work at long control time by Eq. (29) is divided into the mean one

$$W^{(\text{mean})}(\tau) = \frac{\tilde{\omega}(1)}{8\tau^2} \left[ \frac{\tilde{\omega}'(0)^2}{\tilde{\omega}(0)^4} + \frac{\tilde{\omega}'(1)^2}{\tilde{\omega}(1)^4} \right] \sum_{n=0}^{\infty} \left( n + \frac{1}{2} \right) p_n, \quad (32)$$

and the oscillating one

$$W^{(\text{osc})}(\tau) = -\frac{\cos[2\tau\tilde{\varphi}(1)]}{4\tau^2} \frac{\omega'(0)\tilde{\omega}'(1)}{\omega(0)^2\tilde{\omega}(1)} \sum_{n=0}^{\infty} \left( n + \frac{1}{2} \right) p_n. \quad (33)$$

The exact result of the extra work is obtained from the numerical calculation of the nonadiabatic factor with an auxiliary differential equation [37,46,51]. The details are shown in Appendix B.

We calculate the net work  $W_T^{\text{adi}}$  and the heat  $Q_h^{\text{adi}}$  for the quasistatic Otto cycle. Since the population on each state remains unchanged during the quantum adiabatic processes, the internal energy of the four states follows as  $\langle H \rangle_1 = \coth(\beta_h \omega_0/2) \omega_0/2$ ,  $\langle H \rangle_2^{\text{adi}} = \coth(\beta_h \omega_0/2) \omega_1/2$ ,  $\langle H \rangle_3 = \coth(\beta_c \omega_1/2) \omega_1/2$ , and  $\langle H \rangle_4^{\text{adi}} = \coth(\beta_c \omega_1/2) \omega_0/2$ . The net work of the quasistatic cycle is

$$W_T^{\text{adi}} = \frac{\omega_0 - \omega_1}{2} \left[ \coth\left(\frac{\beta_h \omega_0}{2}\right) - \coth\left(\frac{\beta_c \omega_1}{2}\right) \right]. \quad (34)$$

The heat absorbed from the hot source is

$$Q_h^{\text{adi}} = \omega_0 \left[ \coth\left(\frac{\beta_h \omega_0}{2}\right) - \coth\left(\frac{\beta_c \omega_1}{2}\right) \right]. \quad (35)$$

We first adopt the linear protocol  $\tilde{\omega}_l(s) = \tilde{\omega}(0) + [\tilde{\omega}(1) - \tilde{\omega}(0)]s$  for the finite-time adiabatic process. We set the parameters as  $\omega_0 = 2$ ,  $\omega_1 = 1$ , and  $M = 1$ , and choose the temperature for the hot source and cold sink as  $T_h = 5$  and  $T_c = 2$  respectively.

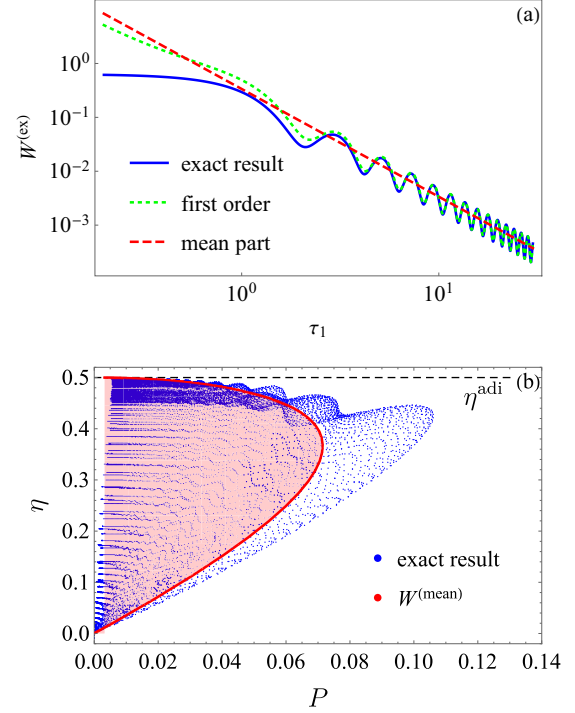


FIG. 6. (a) Extra work in the finite-time adiabatic process  $1 \rightarrow 2$  with the linear protocol  $\tilde{\omega}_l$ . The parameters are chosen as  $\omega_0 = 2$ ,  $\omega_1 = 1$ , and  $M = 1$ , with the temperatures  $T_h = 5$  and  $T_c = 2$ . (b) Reachable power and efficiency for the quantum harmonic Otto engine.

In Fig. 6(a), we compare the first-order result of extra work with the exact numerical result for the finite-time adiabatic process  $1 \rightarrow 2$  with  $\tilde{\omega}(0) = \omega_0$  and  $\tilde{\omega}(1) = \omega_1$ . The first-order adiabatic result (the green dotted curve) matches with the exact numerical result (the blue curve) at long control time. The extra work decreases with oscillation when increasing the control time  $\tau_1$ , retaining the quantum adiabatic limit with infinite control time. Neglecting the oscillation, the extra work satisfies the  $\mathcal{C}/\tau^2$  scaling (red dashed line). Figure 6(b) shows the constraint relation between the efficiency and the power for the finite-time quantum harmonic Otto engine. We set the shortest control time as  $a = 0.02$ . The integers  $j_1$  and  $j_2$  range from 0 to 280, and the control times  $\tau_1$  and  $\tau_3$  range from 0.02 to 78.6. The results are similar to the two-level Otto engine: the oscillating extra work can be utilized to obtain higher maximum power with higher efficiency.

To reduce the extra work in the finite-time adiabatic process at the given control time  $\tau$ , we consider a special protocol [61] given by

$$\tilde{\omega}_s(s) = \frac{\tilde{\omega}(0)}{\left[ \frac{\tilde{\omega}(0)}{\tilde{\omega}(1)} - 1 \right] s + 1}, \quad (36)$$

where  $\tilde{\omega}'(s)/\tilde{\omega}(s)^2 = 1/\tilde{\omega}(0) - 1/\tilde{\omega}(1)$  is a constant. In this special protocol, the extra work by the sum of Eqs. (32) and (33) can approach zero at the specific control time  $\tau = n\pi/\tilde{\varphi}(1)$ ,  $n = 1, 2, \dots$ , with the dynamical phase  $\tilde{\varphi}(1) = [\ln(\tilde{\omega}(0)) - \ln(\tilde{\omega}(1))]/[1/\tilde{\omega}(1) - 1/\tilde{\omega}(0)]$ .

Figure 7 shows the results for the special protocol, with the same parameters chosen in Fig. 6. Figure 7(a) presents the

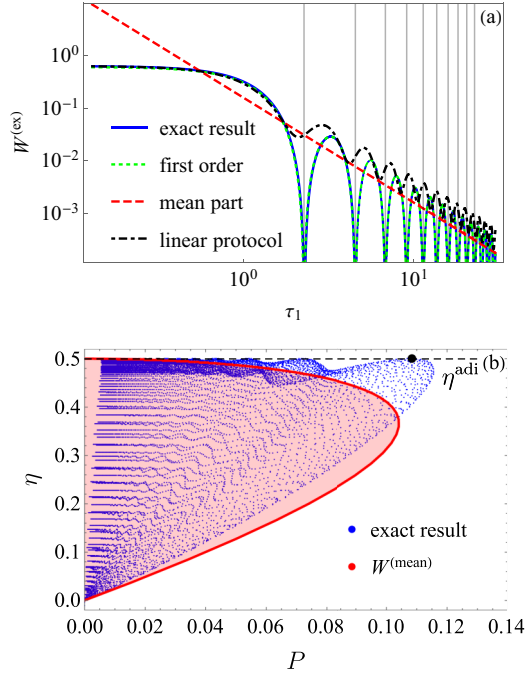


FIG. 7. (a) Extra work for the finite-time adiabatic process  $1 \rightarrow 2$  with the special protocol  $\tilde{\omega}_s$  with different control time  $\tau_1$ . The vertical gray line shows the extra work approaches zero at the specific control time. (b) Reachable power and efficiency for the quantum harmonic Otto engine. All the parameters are chosen the same as in Fig. 6.

first-order result (green dotted curve) and the exact numerical result (blue solid curve) of the extra work, with the exact result of the linear protocol shown as the black dash-dotted curve for comparing. Figure 7(a) clearly shows that the extra work is smaller than that of the linear protocol for most control times  $\tau$ , and can approach zero at the specific control time.

Figure 7(b) shows the constraint between the efficiency and the power for the special protocol. The sampling of control times  $\tau_1$  and  $\tau_3$  is the same as that in Fig. 6(b). When the control time of the two adiabatic processes is chosen as the specific control time  $\tau = n\pi/\tilde{\varphi}(1) = n\pi/(2\ln 2)$ ,  $n = 1, 2, \dots$ , the efficiency approaches the one of the quasistatic Otto cycle (the horizontal black dashed line). For the specific control time  $\tau_1 = \tau_3 = \pi/(2\ln 2)$ , the heat engine gains large power with the quasistatic efficiency, located as the black point. Compared to the linear protocol in Fig. 6(b), the quantum Otto engine with the special protocol attains larger maximum power and higher efficiency.

## V. CONCLUSION

In this paper, we study the effect of the oscillating extra work on both the efficiency and output power of a quantum system with a simple energy-level structure, e.g., the two-level system and the quantum harmonic oscillator. We conclude that the oscillating property of the extra work can be utilized to obtain higher maximum power and higher efficiency at the maximum power for the finite-time quantum Otto engine by elaborately controlling the finite-time adiabatic processes.

We design special control schemes for the finite-time adiabatic process, where the extra work approaches zero at the specific control time. By adopting the special protocol in the finite-time Otto engine, the engines can be optimized to approach the quasistatic efficiency  $\eta^{adi}$  with nonzero output power in finite-time Otto cycle.

*Note added.* Recently, we noticed the implementation of a quantum Otto cycle in experiments [62,63], where the experimental result [62] clearly shows the oscillation in power and efficiency with increasing control time. An analytical result of efficiency and power can be obtained at long control time with our general formalism to match the numerical and experimental results in Ref. [62].

## ACKNOWLEDGMENTS

H.D. thanks D. Z. Xu for helpful discussion. This work is supported by the NSFC (Grants No. 11534002 and No. 11875049), the NSAF (Grants No. U1730449 and No. U1530401), and the National Basic Research Program of China (Grants No. 2016YFA0301201 and No. 2014CB921403). H.D. also thanks The Recruitment Program of Global Youth Experts of China.

## APPENDIX A: TWO-LEVEL SYSTEM

In this Appendix, we give the derivation of the asymptotic amplitude to the first-order adiabatic approximation by Eq. (19). Representing the amplitude  $b_{nl}(s) = c_{nl}(\tau s)$  with the rescaled time parameter  $s$ , Eqs. (15) and (16) are rewritten as

$$\frac{d}{ds}b_{ng} = e^{-2i\tau\tilde{\phi}(s)} \frac{\sin|\theta|}{2\tilde{\Lambda}(s)^2} \frac{d\tilde{\lambda}}{ds} b_{ne}, \quad (\text{A1})$$

$$\frac{d}{ds}b_{ne} = -e^{2i\tau\tilde{\phi}(s)} \frac{\sin|\theta|}{2\tilde{\Lambda}(s)^2} \frac{d\tilde{\lambda}}{ds} b_{ng}. \quad (\text{A2})$$

According to Ref. [60], the solution to the first-order adiabatic approximation is carried out as

$$b_{ge}^{[1]}(s) = \frac{i \sin|\theta|}{4\epsilon\tau} \left[ \frac{\tilde{\lambda}'(s)e^{2i\tau\tilde{\phi}(s)}}{\tilde{\Lambda}(s)^3} - \frac{\tilde{\lambda}'(0)}{\tilde{\Lambda}(0)^3} \right], \quad (\text{A3})$$

$$b_{eg}^{[1]}(s) = \frac{i \sin|\theta|}{4\epsilon\tau} \left[ \frac{\tilde{\lambda}'(s)e^{-2i\tau\tilde{\phi}(s)}}{\tilde{\Lambda}(s)^3} - \frac{\tilde{\lambda}'(0)}{\tilde{\Lambda}(0)^3} \right]. \quad (\text{A4})$$

The amplitude at the end of the finite-time adiabatic process by Eq. (19) follows immediately  $c_{ge}^{[1]}(\tau) = b_{ge}^{[1]}(1)$ .

Next, we give the explicit result for the special protocol  $\tilde{\lambda}_s(s)$ . To allow the extra work approach zero at the specific control time, we design a special protocol by setting  $\tilde{\lambda}'(s)/\tilde{\Lambda}(s)^3 = C$  as a constant at any moment during the finite-time adiabatic process. The constant  $C$  is determined by the initial  $\tilde{\lambda}(0)$  and final value  $\tilde{\lambda}(1)$ . Together with the initial and final conditions, we obtain the implicit function by Eq. (24). In Fig. 8, we compare the special protocol  $\tilde{\lambda}_s$  with the linear protocol  $\tilde{\lambda}_l$ , with the chosen parameters  $\theta = 0.4$ ,  $\epsilon = 1$ ,  $\tilde{\lambda}(0) = 0.1$ ,  $\tilde{\lambda}(1) = 0.8$ . For the the special protocol, we

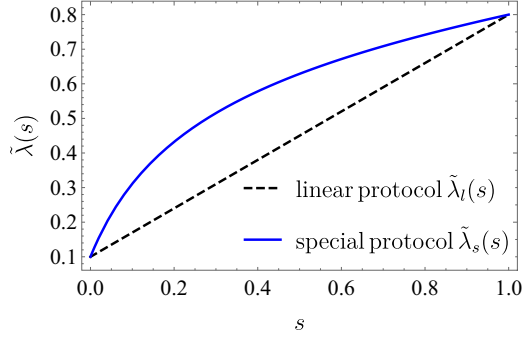


FIG. 8. Two protocols for the two-level system, the lower black dashed line for the linear protocol  $\tilde{\lambda}_l$  and the upper blue solid curve for the special protocol  $\tilde{\lambda}_s$ . The parameters are chosen as  $\tilde{\lambda}(0) = 0.1$ ,  $\tilde{\lambda}(1) = 0.8$ ,  $\theta = 0.4$ .

obtain the dynamical phase at the end of the process as

$$\tilde{\phi}(1) = \frac{\epsilon \sin(\theta) \left[ \arctan \left( \frac{[1+\tilde{\lambda}(1)] \tan \frac{\theta}{2}}{1-\tilde{\lambda}(1)} \right) - \arctan \left( \frac{[1+\tilde{\lambda}(0)] \tan \frac{\theta}{2}}{1-\tilde{\lambda}(0)} \right) \right]}{\frac{\tilde{\lambda}(1) - \cos \theta}{\sqrt{\tilde{\lambda}(1)^2 - 2\tilde{\lambda}(1) \cos \theta + 1}} - \frac{\tilde{\lambda}(0) - \cos \theta}{\sqrt{\tilde{\lambda}(0)^2 - 2\tilde{\lambda}(0) \cos \theta + 1}}}. \quad (\text{A5})$$

The extra work approaches zero at the special control time  $\tau = n\pi / \tilde{\phi}(1)$ ,  $n = 1, 2, \dots$

## APPENDIX B: TIME-DEPENDENT HARMONIC OSCILLATOR

In this Appendix, we give the results of the time-dependent harmonic oscillator, including the first-order adiabatic result and the method for numerical calculation.

Following the method in Ref [60], the differential equation of the amplitude  $c_{nm}(t)$  follows from the Schrödinger equation as

$$\frac{d}{dt} c_{nl}(t) + c_{nl}(t) \langle l | \dot{l} \rangle + \sum_{m \neq l} c_{nm}(t) e^{-i(m-l)\varphi(t)} \langle l | \dot{m} \rangle = 0, \quad (\text{B1})$$

where  $|l\rangle = |l(t)\rangle$  is the instantaneous eigenstate of the time-dependent harmonic oscillator. We rewrite the equation with the rescaled time parameter  $s$  as

$$\frac{d}{ds} b_{nl}(s) + b_{nl}(s) \langle \tilde{l} | \frac{\partial}{\partial s} | \tilde{l} \rangle + \sum_{m \neq l} b_{nm}(s) e^{-i\tau(m-l)\tilde{\varphi}(s)} \langle \tilde{l} | \frac{\partial}{\partial s} | \tilde{m} \rangle = 0, \quad (\text{B2})$$

with  $|\tilde{l}\rangle = |l(s\tau)\rangle$ . With the property of the Hermite polynomial  $H_n(\xi)$ , we obtain the derivative of the instantaneous eigenstate by Eq. (26) as

$$\langle \tilde{m} | \frac{\partial}{\partial s} | \tilde{n} \rangle = \frac{\tilde{\omega}'(s)}{4\tilde{\omega}(s)} (-\sqrt{(n+1)(n+2)}) \delta_{m,n+2}$$

$$+ \sqrt{n(n-1)} \delta_{m,n-2}. \quad (\text{B3})$$

The terms  $\langle \tilde{m} | \frac{\partial}{\partial s} | \tilde{n} \rangle$  with  $m \neq n \pm 2$  are all zero.

According to Ref. [60], we obtain the solution to the first-order adiabatic approximation as

$$b_{n,n+2}^{[1]}(s) = -i \frac{\sqrt{(n+1)(n+2)}}{8\tau} \left( \frac{\tilde{\omega}'(s)}{\tilde{\omega}(s)^2} e^{2i\tau\tilde{\varphi}(s)} - \frac{\tilde{\omega}'(0)}{\tilde{\omega}(0)^2} \right), \quad (\text{B4})$$

and

$$b_{n,n-2}^{[1]}(s) = -i \frac{\sqrt{n(n-1)}}{8\tau} \left( \frac{\tilde{\omega}'(s)}{\tilde{\omega}(s)^2} e^{-2i\tau\tilde{\varphi}(s)} - \frac{\tilde{\omega}'(0)}{\tilde{\omega}(0)^2} \right). \quad (\text{B5})$$

The diagonal term to the first-order adiabatic approximation is  $b_{n,n}^{[1]}(s) = 1$  [60]. The terms  $b_{n,m}^{[1]}(s) = 0$ ,  $m \neq n$ ,  $n \pm 2$  are all zero since  $\langle \tilde{m} | \frac{\partial}{\partial s} | \tilde{n} \rangle = 0$ . The amplitude at the end of the finite-time adiabatic process by Eqs. (30) and (31) follows as  $c_{n,n\pm 2}^{[1]}(\tau) = b_{n,n\pm 2}^{[1]}(1)$ .

In Ref. [46], the exact result of the internal energy during the finite-time adiabatic process is described by the nonadiabatic factor  $\mathcal{N}(t)$  as

$$\langle H(\omega(t)) \rangle = \frac{\omega(t)}{2} \mathcal{N}(t) \coth \left[ \frac{\beta\omega(0)}{2} \right]. \quad (\text{B6})$$

The nonadiabatic factor  $\mathcal{N}(t)$  is determined by a scalar  $c(t)$  as

$$\mathcal{N}(t) = \frac{[\dot{c}(t)]^2 + [\omega(t)]^2 [c(t)]^2 + \frac{[\omega(0)]^2}{[c(t)]^2}}{2\omega(t)\omega(0)}, \quad (\text{B7})$$

where  $c(t)$  satisfies the differential equation

$$\ddot{c}(t) + \omega(t)^2 c(t) = \frac{\omega(0)^2}{c(t)^3}, \quad (\text{B8})$$

with the initial conditions  $c(0) = 1$ ,  $c'(0) = 0$ .

With Eq. (B6), the work during the finite-time adiabatic process is rewritten with  $\mathcal{N}(t)$  as  $W(\tau) = \frac{\omega(\tau)}{2} \mathcal{N}(\tau) \coth \left( \frac{\beta\omega(0)}{2} \right) - \frac{\omega(0)}{2} \coth \left( \frac{\beta\omega(0)}{2} \right)$ . Correspondingly, the quasistatic work is

$$W^{\text{adi}} = \frac{\omega(\tau) - \omega(0)}{2} \coth \left( \frac{\beta\omega(0)}{2} \right), \quad (\text{B9})$$

and the extra work is

$$W^{\text{(ex)}}(\tau) = \frac{\omega(\tau)}{2} [\mathcal{N}(\tau) - 1] \coth \left( \frac{\beta\omega(0)}{2} \right). \quad (\text{B10})$$

It is verified  $\mathcal{N}(\tau) \geq 1$ , which approach 1 for infinite control time  $\tau \rightarrow \infty$ . The difference  $\mathcal{N}(\tau) - 1$  describes the non-adiabatic effect, and does not depend on the initial inverse temperature  $\beta$ . Substituting Eq. (B10) into Eqs. (4) and (5), we rewrite the output power

$$P^h = \frac{[\omega_0 - \omega_1 \mathcal{N}_1(\tau_1)] \coth \left( \frac{\beta_h \omega_0}{2} \right) + [\omega_1 - \omega_0 \mathcal{N}_3(\tau_3)] \coth \left( \frac{\beta_c \omega_1}{2} \right)}{2(\tau_1 + \tau_3)}, \quad (\text{B11})$$



and the corresponding efficiency

$$\eta^h = 1 - \frac{\omega_1 \left[ \mathcal{N}_1(\tau_1) \coth\left(\frac{\beta_h \omega_0}{2}\right) - \coth\left(\frac{\beta_c \omega_1}{2}\right) \right]}{\omega_0 \left[ \coth\left(\frac{\beta_h \omega_0}{2}\right) - \mathcal{N}_3(\tau_3) \coth\left(\frac{\beta_c \omega_1}{2}\right) \right]}, \quad (\text{B12})$$

where  $\mathcal{N}_1(\tau_1)$  and  $\mathcal{N}_3(\tau_3)$  denote the nonadiabatic factors for the two finite-time adiabatic processes. In the numerical calculation, we first choose different control times to obtain the exact result of the nonadiabatic factor  $\mathcal{N}_i(\tau_i)$ ,  $i = 1, 3$  for the two finite-time adiabatic processes by solving Eq. (B8) numerically. Then, we use Eqs. (B11) and (B12) to calculate the exact power and efficiency, respectively.

- 
- [1] K. Maruyama, F. Nori, and V. Vedral, *Rev. Mod. Phys.* **81**, 1 (2009).
- [2] M. Esposito, U. Harbola, and S. Mukamel, *Rev. Mod. Phys.* **81**, 1665 (2009).
- [3] M. Campisi, P. Hänggi, and P. Talkner, *Rev. Mod. Phys.* **83**, 771 (2011).
- [4] P. Strasberg, G. Schaller, T. Brandes, and M. Esposito, *Phys. Rev. X* **7**, 021003 (2017).
- [5] S. Vinjanampathy and J. Anders, *Contemp. Phys.* **57**, 545 (2016).
- [6] M. O. Scully, S. Zubairy, G. S. Agarwal, and H. Walther, *Science* **299**, 862 (2003).
- [7] H. T. Quan, P. Zhang, and C. P. Sun, *Phys. Rev. E* **73**, 036122 (2006).
- [8] P. Solinas and S. Gasparinetti, *Phys. Rev. A* **94**, 052103 (2016).
- [9] G. Francica, J. Goold, and F. Plastina, *Phys. Rev. E* **99**, 042105 (2019).
- [10] F. Benatti, R. Floreanini, and M. Piani, *Phys. Rev. Lett.* **91**, 070402 (2003).
- [11] B. Kraus, H. P. Büchler, S. Diehl, A. Kantian, A. Micheli, and P. Zoller, *Phys. Rev. A* **78**, 042307 (2008).
- [12] F. Altintas, A. U. C. Hardal, and Ö. E. Müstecaplıoğlu, *Phys. Rev. E* **90**, 032102 (2014).
- [13] A. Tavakoli, G. Haack, N. Brunner, and J. B. Brask, [arXiv:1906.00022v1](https://arxiv.org/abs/1906.00022v1).
- [14] J. Jaramillo, M. Beau, and A. del Campo, *New J. Phys.* **18**, 075019 (2016).
- [15] Y.-H. Ma, S.-H. Su, and C.-P. Sun, *Phys. Rev. E* **96**, 022143 (2017).
- [16] J. Bengtsson, M. N. Tengstrand, A. Wacker, P. Samuelsson, M. Ueda, H. Linke, and S. M. Reimann, *Phys. Rev. Lett.* **120**, 100601 (2018).
- [17] J. Chen, H. Dong, and C.-P. Sun, *Phys. Rev. E* **98**, 062119 (2018).
- [18] F. L. Curzon and B. Ahlborn, *Am. J. Phys.* **43**, 22 (1975).
- [19] P. Salamon and R. S. Berry, *Phys. Rev. Lett.* **51**, 1127 (1983).
- [20] M. Esposito, R. Kawai, K. Lindenberg, and C. VandenBroeck, *Phys. Rev. Lett.* **105**, 150603 (2010).
- [21] B. Andresen, *Angew. Chem. Int. Ed.* **50**, 2690 (2011).
- [22] R. S. Whitney, *Phys. Rev. Lett.* **112**, 130601 (2014).
- [23] R. Dann, A. Tobalina, and R. Kosloff, *Phys. Rev. Lett.* **122**, 250402 (2019).
- [24] H. T. Quan, Y. X. Liu, C. P. Sun, and F. Nori, *Phys. Rev. E* **76**, 031105 (2007).
- [25] Z. C. Tu, *J. Phys. A: Math. Theor.* **41**, 312003 (2008).
- [26] B. Rutten, M. Esposito, and B. Cleuren, *Phys. Rev. B* **80**, 235122 (2009).
- [27] A. Alecce, F. Galve, N. L. Gullo, L. Dell'Anna, F. Plastina, and R. Zambrini, *New J. Phys.* **17**, 075007 (2015).
- [28] N. Shiraishi, K. Saito, and H. Tasaki, *Phys. Rev. Lett.* **117**, 190601 (2016).
- [29] S. Deffner, *Entropy* **20**, 875 (2018).
- [30] T. Schmiedl and U. Seifert, *EPL* **81**, 20003 (2007).
- [31] V. Cavina, A. Mari, and V. Giovannetti, *Phys. Rev. Lett.* **119**, 050601 (2017).
- [32] A. Ryabov and V. Holubec, *Phys. Rev. E* **93**, 050101(R) (2016).
- [33] R. Long and W. Liu, *Phys. Rev. E* **94**, 052114 (2016).
- [34] V. Holubec and A. Ryabov, *J. Stat. Mech.: Theory Exp.* (2016) 073204.
- [35] Y.-H. Ma, D. Xu, H. Dong, and C.-P. Sun, *Phys. Rev. E* **98**, 022133 (2018).
- [36] Y.-H. Ma, D. Xu, H. Dong, and C.-P. Sun, *Phys. Rev. E* **98**, 042112 (2018).
- [37] O. Abah, J. Roßnagel, G. Jacob, S. Deffner, F. Schmidt-Kaler, K. Singer, and E. Lutz, *Phys. Rev. Lett.* **109**, 203006 (2012).
- [38] J. Roßnagel, O. Abah, F. Schmidt-Kaler, K. Singer, and E. Lutz, *Phys. Rev. Lett.* **112**, 030602 (2014).
- [39] B. Karimi and J. P. Pekola, *Phys. Rev. B* **94**, 184503 (2016).
- [40] A. Insinga, B. Andresen, and P. Salamon, *Phys. Rev. E* **94**, 012119 (2016).
- [41] M. Campisi and R. Fazio, *Nat. Commun.* **7**, 11895 (2016).
- [42] R. Kosloff and Y. Rezek, *Entropy* **19**, 136 (2017).
- [43] P. A. Erdman, V. Cavina, R. Fazio, F. Taddei, and V. Giovannetti, [arXiv:1812.05089](https://arxiv.org/abs/1812.05089).
- [44] T. Denzler and E. Lutz, [arXiv:1907.02566v1](https://arxiv.org/abs/1907.02566v1).
- [45] P. A. Camati, J. F. G. Santos, and R. M. Serra, *Phys. Rev. A* **99**, 062103 (2019).
- [46] X. Chen, A. Ruschhaupt, S. Schmidt, A. del Campo, D. Guéry-Odelin, and J. G. Muga, *Phys. Rev. Lett.* **104**, 063002 (2010).
- [47] J. Deng, Q.-H. Wang, Z. Liu, P. Hänggi, and J. Gong, *Phys. Rev. E* **88**, 062122 (2013).
- [48] A. del Campo, *Phys. Rev. Lett.* **111**, 100502 (2013).
- [49] A. del Campo, J. Goold, and M. Paternostro, *Sci. Rep.* **4**, 6208 (2014).
- [50] O. Abah and E. Lutz, *Phys. Rev. E* **98**, 032121 (2018).
- [51] A. del Campo, A. Chenu, S. Deng, and H. Wu, in *Fundamental Theories of Physics* (Springer International, Berlin, 2018), pp. 127–148.

- [52] S. Deng, A. Chenu, P. Diao, F. Li, S. Yu, I. Coulamy, A. del Campo, and H. Wu, *Sci. Adv.* **4**, eaar5909 (2018).
- [53] B. Çakmak and Ö. E. Müstecaplıoğlu, *Phys. Rev. E* **99**, 032108 (2019).
- [54] L. Chotorlishvili, M. Azimi, S. Stagraczyński, Z. Toklikishvili, M. Schüler, and J. Berakdar, *Phys. Rev. E* **94**, 032116 (2016).
- [55] S. Su, J. Chen, Y. Ma, J. Chen, and C. Sun, *Chin. Phys. B* **27**, 060502 (2018).
- [56] C.-P. Sun, *J. Phys. A: Math. Gen.* **21**, 1595 (1988).
- [57] F. Wilczek and A. Shapere, *Geometric Phases in Physics* (World Scientific, Singapore, 1989).
- [58] C.-P. Sun, *Phys. Rev. D* **41**, 1318 (1990).
- [59] G. Rigolin, G. Ortiz, and V. H. Ponce, *Phys. Rev. A* **78**, 052508 (2008).
- [60] J.-F. Chen, C.-P. Sun, and H. Dong, [arXiv:1904.12128v1](https://arxiv.org/abs/1904.12128v1).
- [61] S. Deng, Z.-Y. Shi, P. Diao, Q. Yu, H. Zhai, R. Qi, and H. Wu, *Science* **353**, 371 (2016).
- [62] J. P. S. Peterson, T. B. Batalhão, M. Herrera, A. M. Souza, R. S. Sarthour, I. S. Oliveira, and R. M. Serra, [arXiv:1803.06021v1](https://arxiv.org/abs/1803.06021v1).
- [63] R. J. de Assis, T. M. de Mendonça, C. J. Villas-Boas, A. M. de Souza, R. S. Sarthour, I. S. Oliveira, and N. G. de Almeida, *Phys. Rev. Lett.* **122**, 240602 (2019).